Distant iron-shallow-donor pairs in silicon detected by electron paramagnetic resonance

M. Höhne, U. Juda, and H. Riemann

Institut für Kristallzüchtung Berlin-Adlershof, Rudower Chaussee 6, D-12489 Berlin, Germany

J.-M. Spaeth and S. Greulich-Weber

Universität-Gesamthochschule Paderborn, Fachbereich Physik, D-33095 Paderborn, Germany

(Received 3 February 1994)

The electron-paramagnetic-resonance transitions of isolated neutral interstitial iron ($Fe_i{}^0$) in n-type silicon show a satellite structure, which is clearly detectable for donor concentrations (P or As, respectively) above 10^{15} cm^{-3}. The satellite structure reflects the hyperfine interaction with one shallow-donor nucleus and one iron nucleus in the case of doping with ^{57}Fe. The spectra are explained by the spin-spin interaction of one $Fe_i{}^0$ (spin $S_{Fe} = 1$) and one shallow donor (spin $S_D = \frac{1}{2}$). Neither line positions nor line shapes depend on the direction of the magnetic field with respect to the crystal axes. A random distribution of distant iron-donor pairs is suggested by the following facts. Both $(S_{Fe} + S_D)$ levels (high-field satellites) and $(S_{Fe}\text{-}S_D)$ levels (low-field satellites) are thermally populated. Asymmetric line shapes and dissimilar hyperfine components indicate a continuous distribution of spin-spin interaction parameters.

INTRODUCTION

Iron as a scarcely avoidable contaminant in silicon influencing essential properties and degradation of devices has been thoroughly investigated by various methods.[1] Its relevance has recently been underlined by investigation of polycrystalline silicon for photovoltaic applications.[2]

A large number of iron-related defects in silicon have been thoroughly investigated by electron paramagnetic resonance (EPR); they have been quoted in a survey[3] containing spectroscopic parameters. Besides various complex defects, isolated interstitial ions are known[4] in two charge states $Fe_i{}^0$ and $Fe_i{}^+$. The easily detectable $Fe_i{}^0$ defect was especially a subject of further EPR (Refs. 5–9) and electron-nuclear double resonance[10,11] investigations. The EPR spectra could be explained in the following way: Neutral interstitial iron has a $3d$ (Ref. 8) configuration. The free-ion ^3F state is split by the cubic crystal field, where at an interstitial site an orbital singlet $^3A_2$ is lower than two excited triplet levels $^3T_2$ and $^3T_1$. Because of the electron spin $S_{Fe} = 1$, a random strain-induced zero-field splitting causes an angular-dependent line broadening for the single-quantum transitions (SQT). The narrow lines of the double-quantum transitions (DQT) exhibit an angular-dependent superhyperfine structure due to ^{29}Si ligands.

The interstitial Fe donor ($E_v + 0.40$ eV), mobile even near room temperature, forms several paramagnetic complex defects with shallow and deep acceptors (see, e.g., Refs. 1 and 12). The occurrence of defect reactions of iron with shallow donors was recently inferred from EPR measurements by comparing $Fe_i{}^0$ concentrations after different thermal treatments of Fe-doped n-type Si.[13] The phenomenon of Fe gettering by surface layers containing high P concentrations was explained by the gettering activity of structural defects.[14] An early EPR study of metallic Si:P with iron concerned relaxation phenomena of conduction-electron spin resonance.[15] In no case were EPR spectra of Fe–shallow-donor complexes reported.

Donor "clusters" are known to cause additional lines between the hyperfine components of the P resonance in Si containing shallow donors in the concentration range of $1 \times 10^{16} - 1 \times 10^{18}$. These clusters are randomly distributed distant pairs and triads, which were experimentally and theoretically investigated.[16–18]

In this paper we contribute an experimental phenomenon to this field of problems by presenting EPR spectra which exhibit a hyperfine structure due to one Fe nucleus as well as to one shallow-donor nucleus. The latter fact induced the term "pair" in the title, though according to the following analysis the two partners are distant neighbors in a diluted random distribution.

EXPERIMENT

Different n-type starting materials were used: Czochralski (CZ) and float zone (FZ) Si with P concentrations c_P of 5×10^{13} cm^{-3} up to 3×10^{16} cm^{-3} P, and FZ Si containing 1×10^{16} cm^{-3} up to 5×10^{17} cm^{-3} As. The samples (roughly $3 \times 3 \times 10$ mm^3) were doped by annealing them at 1200 °C in an evacuated ampoule together with metallic natural Fe or ^{57}Fe, respectively, followed by a rapid quench to room temperature. The way of quenching was modified, and the samples were stored for some days or even months at room temperature; the results did not depend on these treatments apart from slight changes in the concentration of incorporated isolated interstitial iron and in the broadening of the SQT due to modified local stress fields. EPR measurements were done with a Bruker spectrometer ESP 300 with sample temperatures ranging from 4 to 30 K.

EXPERIMENTAL RESULTS

A. EPR spectra

All the samples doped with P and Fe gave the well-known EPR spectra shown in Fig. 1 for two directions of the magnetic field B with respect to the cubic axes. The temperature was $T=20$ K, the microwave power $W=3.17$ mW, and the modulation amplitude $B_{mod}=0.2$ mT. There are hyperfine pair lines caused by the 100% abundant nuclear spin $I=\frac{1}{2}$ of P at fields corresponding to the g value of $g=1.9985$; between them are lines due to exchange coupling of two or three P atoms (according to P concentration) and the Fe_i^0 line at $g=2.0699$ [called central line (CL) in the following] with its angular-dependent linewidth. The DQT as a part of the CL is not visible as a distinct narrow line because we applied larger modulation amplitudes in order to improve the signal-to-noise ratio of the satellites.

In samples containing a sufficiently high concentration of phosphorus, which means more than roughly 1×10^{15} cm^{-3}, the Fe_i^0 CL exhibits a satellite structure of four lines, visible in Fig. 1. The satellite intensities exhibit a roughly linear increase with increasing P concentration c_P; the example of Fig. 1 corresponds to 1×10^{16} cm^{-3}. The satellite structure is isotropic: Neither line positions nor line shapes or intensities depend on the direction of B within the margins of experimental error. The satellite line positions are also independent of temperature and microwave power, whereas these parameters remarkably influence the line shapes and the intensities. Figure 2 gives a 20-K spectrum for an intermediate level of microwave power. It demonstrates that the phenomenon is easily observed on applying suitable conditions of measurement. The field positions B_{o-}, B_{i-}, B_{o+}, and B_{i+}
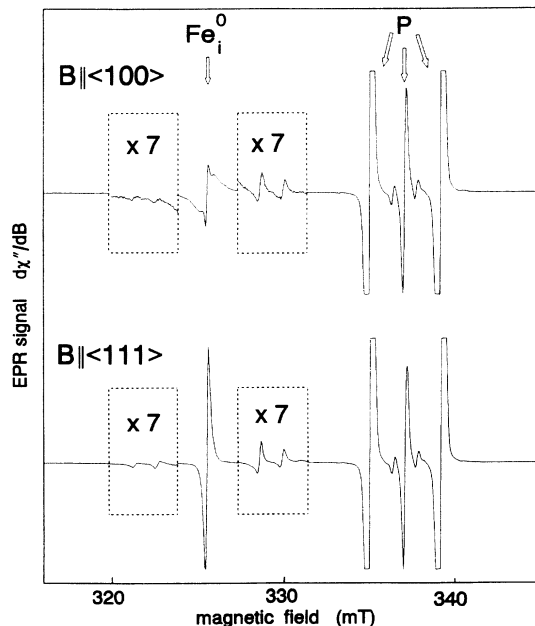
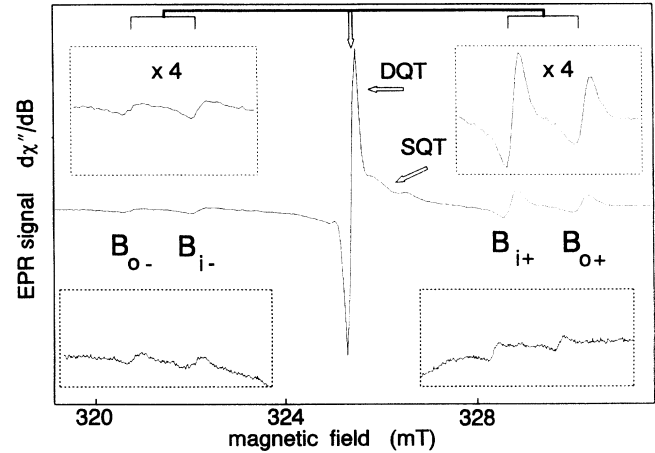

FIG. 2. EPR spectrum at 20 K for $B\|\langle100\rangle$ of Fe_i^0 (SQT and DQT) in Si:P with outer satellites (B_{o-} and B_{o+}) and inner ones (B_{i-} and B_{i+}). $W=3.17$ mW; $B_{mod}=0.2$ mT; $c_P=3\times10^{16}$ cm^{-3}. Satellite positions are indicated by the scheme above the spectrum. The zoomed parts shown in the upper insets underline the asymmetries and different intensities of the satellites. The lower insets represent these spectral parts measured at 7 K.

are specified by the subscripts − and + for the low-field satellites and the high-field ones, and by the subscripts o and i for the outer pair and the inner one, respectively. At high temperature (20 K, 25 K) and low power the satellite lines are of asymmetric shape and of different intensities increasing in the sequence given above (see zoomed parts in the upper insets). With decreasing temperature and increasing microwave power the satellites tend to become more symmetric and of nearly equal intensity; the lower insets of Fig. 2 show the satellites observed at 7 K.

Samples of the same starting materials were doped with iron enriched with the isotope ^{57}Fe (nuclear spin $I=\frac{1}{2}$). The abundance of ^{57}Fe was determined from a measurement of the narrow-line-ligand hyperfine groups of the DQT to be 94%. Figure 3 represents the spectrum
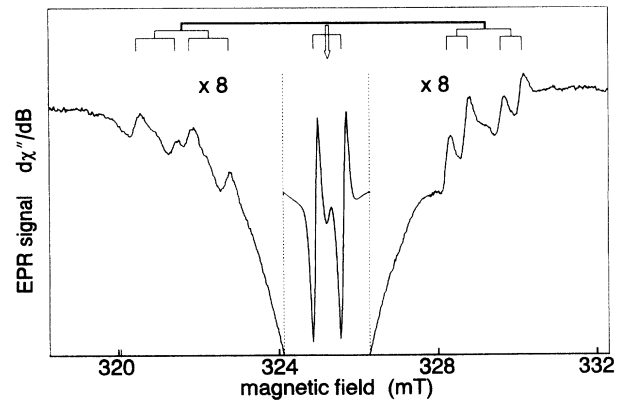

FIG. 1. EPR spectra of Fe_i^0 and P at 20 K for $B\|\langle100\rangle$ and $B\|\langle111\rangle$. $W=3.17$ mW; $B_{mod}=0.2$ mT; $c_P=1\times10^{16}$ cm^{-3}.

FIG. 3. EPR spectrum at 7 K for $B\|\langle100\rangle$ of Fe_i^0 in a sample enriched with ^{57}Fe (94%). $W=3.17$ mW; $B_{mod}=0.2$ mT; $c_P=3\times10^{16}$ cm^{-3}. Satellite positions are indicated by the scheme above the spectrum.

of such a sample in a measurement at 12 K (at 20 K the low-field satellite intensities are smaller compared to the high-field ones, just as in the case of Figs. 1 and 2). The hyperfine splitting of the CL agrees with the value of $|A_{Fe}|=7.0\times10^{-4}$ cm^{-1} known from the literature.[4] The satellites are split because of the interaction with one iron nucleus; but the splittings of the low-field satellites differ strongly from those of the high-field ones.

B. Analysis of EPR spectra

The satellite spectra correspond to a spin Hamiltonian

$$\mathcal{H}=\mathcal{H}_a+\mathcal{H}_b+\mathcal{H}_c \ , \tag{1}$$

with a spin-spin interaction part

$$\mathcal{H}_a=J\mathbf{S}_{Fe}\cdot\mathbf{S}_D \ , \tag{2}$$

a Zeeman part

$$\mathcal{H}_b=\beta(g_{Fe}\mathbf{S}_{Fe}+g_D\mathbf{S}_D)\cdot\mathbf{B} \ , \tag{3}$$

and a hyperfine part

$$\mathcal{H}_c=A_{Fe}\mathbf{S}_{Fe}\cdot\mathbf{I}_{Fe}+A_D\mathbf{S}_D\cdot\mathbf{I}_D \ , \tag{4}$$

with the usual meanings of the symbols. Subscript Fe refers to iron with $S_{Fe}=1$ and $I_{Fe}=\frac{1}{2}$ for ^{57}Fe and $I_{Fe}=0$ for the other isotopes. Subscript D refers to the shallow donor phosphorus with $S_D=\frac{1}{2}$ and $I_D=I_P=\frac{1}{2}$ in a natural abundance of 100%. All the interactions are isotropic.

Neglecting the satellite line-shape distortions, the positions are characterized by the schemes above the spectra in Figs. 2 and 3. These positions follow from the spin Hamiltonian (1) in the limit of strong spin-spin interaction. The wave functions are determined by the electron-spin quantum numbers M_j and by the nuclear-spin quantum numbers m_j with $j=$ Fe, D and

$$|M_{Fe}m_{Fe}M_Dm_D\rangle=|M_{Fe}m_{Fe}\rangle|M_Dm_D\rangle \ . \tag{5}$$

A strong spin-spin interaction H_a yields a twofold level

$$E_1^0=E_2^0=-J \ , \tag{6}$$

related to eigenfunctions

$$a_1|-1m_{Fe}+\tfrac{1}{2}m_D\rangle+b_1|0m_{Fe}-\tfrac{1}{2}m_D\rangle$$

and

$$a_2|+1m_{Fe}-\tfrac{1}{2}m_D\rangle+b_2|0m_{Fe}+\tfrac{1}{2}m_D\rangle \ ,$$

with

$$a_1=a_2=-\sqrt{\tfrac{2}{3}} \ \text{and} \ b_1=b_2=1/\sqrt{3} \ ,$$

and a fourfold level

$$E_3^0=E_4^0=E_5^0=E_6^0=J/2 \ , \tag{7}$$

related to eigenfunctions

$$|+1m_{Fe}+\tfrac{1}{2}m_D\rangle \ ,$$

$$a_4|+1m_{Fe}-\tfrac{1}{2}m_D\rangle+b_4|0m_{Fe}+\tfrac{1}{2}m_D\rangle \ ,$$

$$a_5|-1m_{Fe}+\tfrac{1}{2}m_D\rangle+b_5|0m_{Fe}-\tfrac{1}{2}m_D\rangle \ ,$$

$$|-1m_{Fe}-\tfrac{1}{2}m_D\rangle \ ,$$

with

$$a_4=a_5=1/\sqrt{3} \ \text{and} \ b_4=b_5=\sqrt{\tfrac{2}{3}} \ .$$

With these functions the eigenvalues E_j^1 $(j=1-6)$ of the terms (3) and (4) are calculated, and the energy differences within the multiplets for allowed transitions are

$$E_1^1-E_2^1=\beta(\tfrac{4}{3}g_{Fe}-\tfrac{1}{3}g_D)B+(\tfrac{4}{3}m_{Fe}A_{Fe}-\tfrac{1}{3}m_DA_D) \tag{8}$$

and

$$E_3^1-E_4^1=E_4^1-E_5^1=E_5^1-E_6^1$$
$$=\beta(\tfrac{2}{3}g_{Fe}+\tfrac{1}{3}g_D)B+(\tfrac{2}{3}m_{Fe}A_{Fe}+\tfrac{1}{3}m_DA_D) \ . \tag{9}$$

The quantum numbers are $m_{Fe}=\pm\frac{1}{2}$, for ^{57}Fe, $m_{Fe}=0$ for the other isotopes, and $m_D=m_P=\pm\frac{1}{2}$ for phosphorus. Within experimental error the values of the parameters are those of the isolated defects:[4,19,20]

$$g_{Fe}=2.0699\pm0.0001 \ ;$$

$$g_D=g_P=1.9985\pm0.0001 \ ;$$

$$|A_{Fe}|=(7.0\pm0.1)\times10^{-4} \ \text{cm}^{-1} \ ;$$

$$|A_D|=|A_P|=(39.2\pm0.2)\times10^{-4} \ \text{cm}^{-1} \ .$$

In the case of a strong antiferromagnetic coupling $(J>0)$ only the doublet level would be occupied. The experimental spectra show that both the twofold level and the fourfold level are thermally populated in our experiments.

Although the agreement of the parameters seems to be convincing, we tried to compare with another shallow donor, and prepared a single crystal of Si with suitable concentrations of arsenic. The results are presented in Fig. 4(a) for natural iron and in Fig. 4(b) for iron enriched with ^{57}Fe. The spectra do not exhibit the good signal-to-noise ratios of the P-doped material and the satellites are partly covered by hyperfine components and donor cluster lines, due to the high content of As. But the results were well reproducible and the splitting schemes above the spectra in Fig. 4 follow exactly the formalism of Eqs. (1)–(9). Of course the parameters of P had to be replaced by those of As:[19,20]

$$I_D=I_{As}=\tfrac{3}{2} \ ; \quad m_D=m_{As}=\pm\tfrac{1}{2},\pm\tfrac{3}{2} \ ;$$

$$g_D=g_{As}=1.9986\pm0.0001 \ ;$$
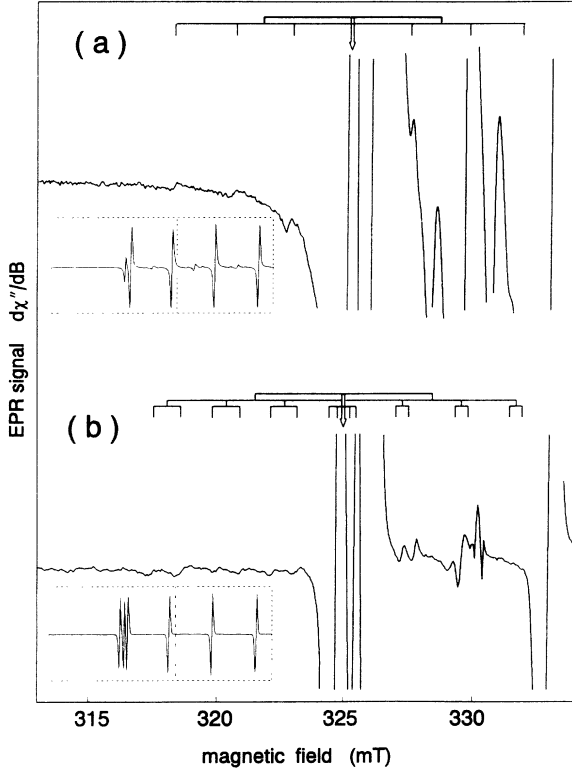
$$|A_D|=|A_{As}|=(66.2\pm0.02)\times10^{-4}\text{cm}^{-1} \ .$$

FIG. 4. EPR spectra at 20 K for $B||\langle 111 \rangle$ of Fe_i^0 in Si:As. $W=3.17$ mW; $B_{mod}=0.2$ mT. (a) Doped with natural Fe, $c_{As}\sim1\times10^{17}$ cm^{-3}. (b) Doped with 94% ^{57}Fe, $c_{As}\sim3\times10^{16}$ cm^{-3}. The zoomed spectra are the left parts of the total spectra shown in the insets.
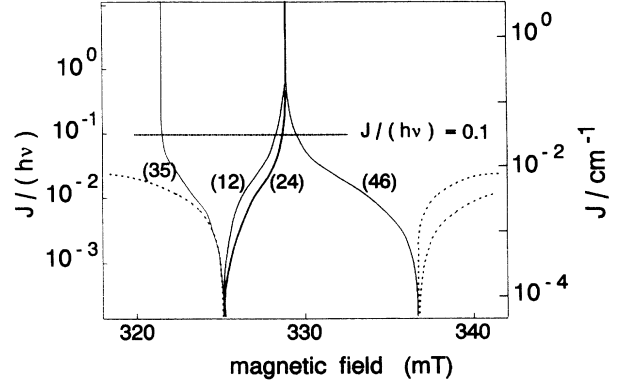

FIG. 5. Central positions of satellite hyperfine groups calculated in dependence of spin-spin interaction for $D=0$. Low-intensity lines are indicated by dashed lines. For the marked value of $J/(h\nu)$ the dependences on D will be given in Fig. 7.

DISCUSSION

The theory of systems coupled by spin-spin interaction has recently been summarized;[21] the collection of examples is now extended by the important system of iron in n-type silicon. We will discuss the geometrical arrangement of iron-donor pairs; therefore, a quantitative estimate will be given in the following.

In the report of the experimental results, the assumption of a spin-spin interaction gave a correct explanation of the line positions. On the other hand, the fact that both line groups corresponding to the fourfold level and to the twofold one are observed in the spectra verifies the thermal population of both levels even at low temperatures. This means that the spin-spin interactions are not as large as usually observed for close partners.[21] Therefore, we will now treat Zeeman interaction (3) and spin-spin interaction (2) as having equal order of magnitude; the corresponding matrix with functions (5) is diagonalized. Eigenfunctions of type (6) and (7) are obtained with coefficients a_j and b_j ($j=2,3,4,5$) depending on the relative magnitude of Zeeman interaction and spin-spin interaction. Probabilities P_{jk} ($j,k=1-6$) of microwave-induced transitions between the six states are calculated in the usual way for each value of the spin-spin interaction parameter J. The result is represented in Fig. 5. The field positions of the strongly allowed transitions are

given by full lines labeled by index pairs $jk=12, 24, 46$, and 35 in parentheses; line (24) is the most intense one. Resonances with negligible transition probabilities are indicated by dashed lines. The right-hand scale shows the value of J for $h\nu=0.314$ cm^{-1} corresponding to the microwave frequency of our experiments [energies E are given as wave numbers $E/(hc)$]. The resonance fields of the isolated Fe_i^0 and P defects are approached at the bottom of the figure.

The left-hand scale of Fig. 5 visualizes the fact that the resonance fields of strong spin-spin interaction (upper part of the figure) are also observed for values of J even slightly smaller than the microwave energy. Thus, a nearly equal thermal population of all the levels even at 7 K is natural for this range of J values. The intensity of the absorption line corresponding to a transition $j\leftrightarrow k$ is proportional to the product

$$I_{jk}=P_{jk}(n_j-n_k) , \tag{10}$$

where the thermal occupation of the level j characterized by the fraction n_j is assumed to be restricted to the six levels considered above:

$$\sum_{j=1}^{6} n_j=1 .$$

Figure 6 represents the calculated ratio γ of the high-field satellites' intensity to the intensity of the low-field ones. Part (a) of the figure gives the ratio

$$\gamma=(I_{12}+I_{24}+I_{46})/I_{35} ,$$

typical for the case of coincident or nearly coincident field positions of the high-field satellites. Part (b) gives the ratio

$$\gamma=I_{24}/I_{35} ,$$

possibly of interest in the case of strain-shifted lines (12) and (46) (see below). As expected, the levels of the excited states are not occupied ($\gamma=0$) for values of roughly $J/(h\nu)>70$, i.e., only the low-field satellites are observed. For $J/(h\nu)<1$ the levels are equally populated.
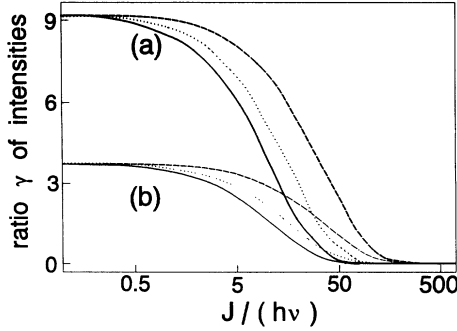
FIG. 6. Calculated intensity ratio γ of high-field and low-field satellites, respectively, for 7 K (solid lines), 12 K (dotted lines), and 25 K (dashed lines). In (a) all fine-structure transitions are included, in (b) it is only the central one.

Up to now only isotropic interactions (2)–(4) were considered as corresponding to the experimental behavior. On the other hand, it is known that anisotropic interactions exist:[22,21] a fine-structure contribution

$$\mathcal{H}_d = \mathbf{S}_{Fe} \cdot \mathbf{D} \cdot \mathbf{S}_{Fe} \tag{11}$$

of the $S_{Fe} = 1$ state, and a magnetic dipole-dipole interaction

$$\mathcal{H}_e = \beta^2 g_{Fe} g_D r^{-3} [\mathbf{S}_{Fe} \cdot \mathbf{S}_D - 3r^{-2}(\mathbf{S}_{Fe} \cdot \mathbf{r})(\mathbf{S}_D \cdot \mathbf{r})] , \tag{12}$$

where $\mathbf{r}$ is the vector from the Fe ion to the P atom, and r is the corresponding distance. It is useful to check the conditions which make these interactions negligible in our experiments.

The crystal-field splitting due to random strains causing the line broadening of the SQT of the Fe_i^0 defect may be exceeded by that due to the strains caused by near-donor defects. For phosphorus-induced strain in Si the fine-structure tensor $\mathbf{D}$ can be calculated approximately following ideas and data contained in early papers[5,23] devoted to this field. For an estimate of the magnitude we confine ourselves to the special case of a point defect located on one of the cubic axes. Thus the fine-structure term (11) is simplified to an axial "quadrupole" term

$$\mathcal{H}_d = D[S_z^2 - S(S+1)/3] . \tag{11a}$$

With the further confinement of $\mathbf{B} \| z$, which yields only diagonal contributions of the term (11a), the influence of the fine-structure term is demonstrated in Fig. 7 for $J/(h\nu) = 0.1$ and 70. These values roughly limit the range relevant to the satellites: For values $J/(h\nu) < 0.1$ the line positions differ essentially from the experimentally observed ones (see Fig. 5), and for $J/(h\nu) > 70$ only the low-field satellites would be observed (see Fig. 6). For the following discussion one learns from Fig. 7 that for values of roughly $|D| < 10 \times 10^{-4}$ cm^{-1} influences of strains can be neglected in the whole range of J. Large values of J cause remarkable line shifts, which are anisotropic according to the type of the interaction (11). For large J and large $|D|$ expected for close neighbors, this shift concerns only the outer members of the high-field satellites. These members [index pairs (12) and (46) in
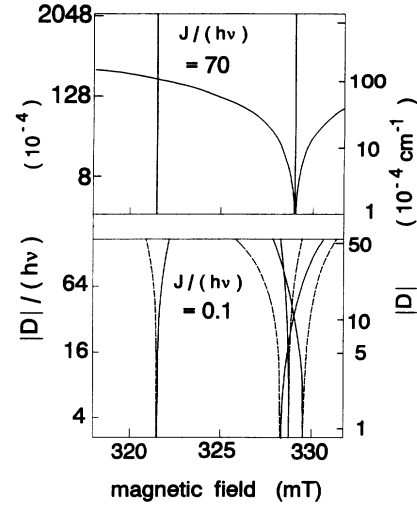

FIG. 7. Central positions of satellite hyperfine groups calculated in dependence of D (solid lines for $D < 0$, broken lines for $D > 0$) for two values of spin-spin interaction.

Fig. 5] shifted far from the central field position might escape from detection. The two other satellite lines keep their field positions and their isotropic behavior; their relative intensities would follow part (b) of Fig. 6. Obviously this is not an argument against a definite close-pair arrangement of Fe_i^0 and shallow donors.

The magnitude of D caused by elastic deformation due to phosphorus in silicon in a distance of r is approximately given by

$$D = -9.48 \text{ cm}^{-1} \left[\frac{r}{10^{-8} \text{ cm}^{-1}} \right]^{-3} \tag{11b}$$

(see the Appendix).

For a distance of $r = 5.43 \times 10^{-8}$ cm^{-1} corresponding to third-nearest neighbors located on a cubic axis, one obtains $D = -0.6$ cm^{-1}. Though approximation (11b) does not yield correct values for near neighbors, it should give the right order of magnitude and can be compared with the value of $|D| = 2.7$ cm^{-1} determined for iron-boron pairs.[4,24] For a distribution of pair distances, the parameter D estimated by relation (11a) will be represented in Fig. 8. It turns out that for a random distribution of pairs, the anisotropic influence of strain fields is beyond the detection limit for the concentrations contained in our samples, which agrees with the experimental results.

The asymmetric line shapes of the satellites (see Figs. 1 and 2) hint at a distribution of J values due to a distribution of "pair" distances. Random distributions of pairs, triads, and larger clusters of exchange-coupled donors in Si had been treated by Poisson statistics.[16–18] For pairs considered here we preferred the following simple treatment. The probability of finding a P atom in a small volume element is the product of this volume times the volume concentration of P, which is assumed to be larger than the concentration of Fe_i^0 ions. Starting from the position of an Fe_i^0 defect, subsequent spheric shells of radius r were considered as volume elements. The probabil-
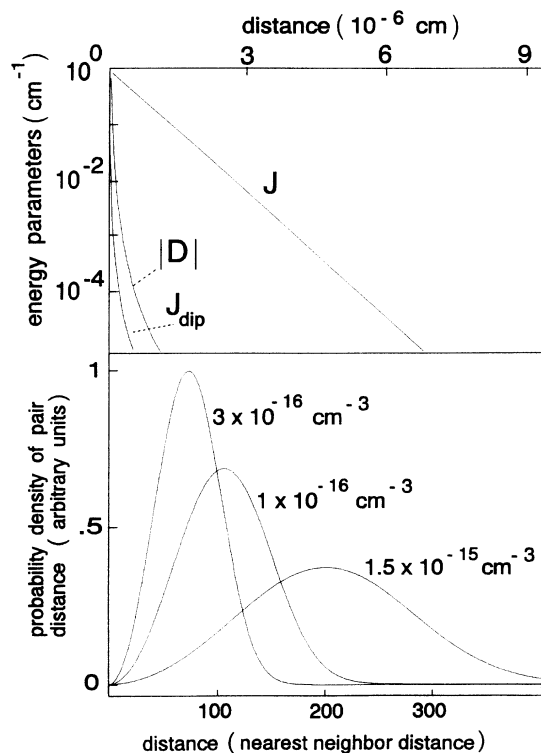
FIG. 8. Energy parameters and probability densities vs distance of interacting partners.

naturally smaller than the experimental ones. The experimental spectra of the Si:P, Fe samples were fitted with

$$J_0 = 0.93 \text{ cm}^{-1} , \quad a = 2.5 \times 10^{-7} \text{ cm} .$$

The value of J_0 is three orders of magnitude smaller than that of interacting identical partners in the P-P pairs ($J_0 = 900 \text{ cm}^{-1}$), whereas the decrease with distance is slower ($a = 1.0 \times 10^{-7}$ cm for P-P pairs).[18]

Criteria for the fit were the relative intensities of the satellites in the spectra for the range of P concentrations (1.5×10^{15} to $3 \times 10^{16} \text{ cm}^{-3}$) in the 18- and 25-K spectra, respectively, and the asymmetric line shapes of the satellites. A decrease of the intensities of the high-field satellites with decreasing temperature compared to the intensities of the low-field satellites is expected for antiferromagnetic coupling caused by a depopulation of the excited fourfold level. Although this is a hint at an antiferromagnetic type of coupling, the depopulation calculated for 7 K is essentially smaller than the observed change in satellite intensities with temperature (see Fig. 2); we suppose that saturation effects are responsible for this phenomenon, which is supported by the fact that increasing the microwave power produces the same tendency as lowering the temperature.

Figure 9 shows simulated spectra for doping with natural iron [part (a) with one Fe_i^0 CL] and with ^{57}Fe enriched according to our experimental conditions [part (b) with two hyperfine components of the Fe_i^0 CL]. Characteristic features are well reflected: Relative intensities cor-

ity of finding a P donor first in a certain shell is the product of the probability that there is a donor in this shell times the probability that there was no donor in all the shells with smaller radii. The resulting probability distribution for pair distances is represented in the lower part of Fig. 8 for three P concentrations applied in our experiments. The upper part Fig. 8 represents interaction parameters versus pair distance. $J_{\text{dip}} = \beta^2 g_{\text{Fe}} g_D r^{-3}$ is the parameter, which gives the dipole-dipole interaction (12) apart from an angular-dependent factor of order 1. Obviously a dipole-dipole interaction is too small to allow an interpretation of the experimental results.

For the isotropic exchange-interaction parameter J we examined a dependence as

$$J = J_0 \exp(-r/a) . \tag{13}$$

A computer simulation was done following the treatment developed above. Corresponding to the different donor concentrations, the probability distribution of J values (see Fig. 8) was considered. For each value of J the eigenvalue problem was solved with (2) and (3); resonance fields and relative intensities I_{jk} were calculated. The hyperfine interaction (4) was included as a perturbation. Shortcomings of our simulation were the assumption of one common linewidth, even for Fe_i^0 with its SQT and its modulation-broadened DQT, and the neglect of P atoms, which are not first neighbors of an Fe_i^0 ion. The latter restriction might easily have been avoided, but in our opinion the consequences of the model are more obvious with this neglect. Thus, the calculated P lines were
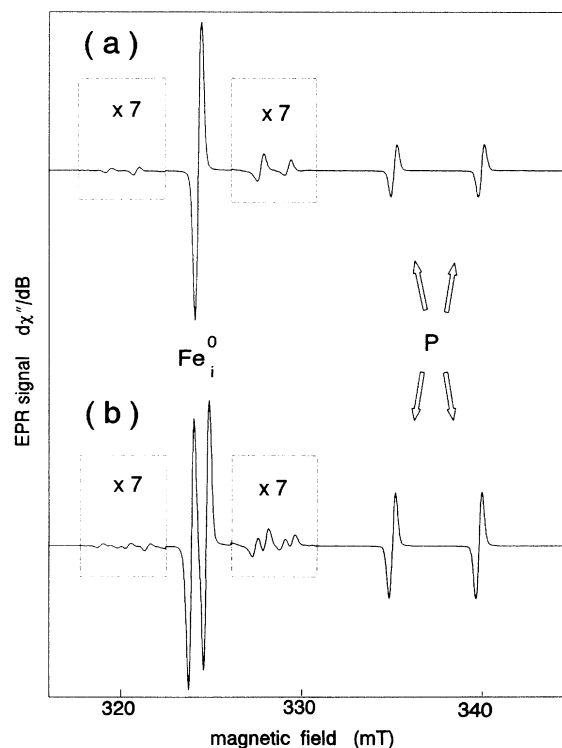

FIG. 9. Calculated spectra for $T = 25$ K, $c_P = 1 \times 10^{16} \text{ cm}^{-3}$ (only interacting P included, see text); (a) natural mixture of iron isotopes; (b) 94% content of ^{57}Fe.

respond to the experimental spectra. This concerns the ratio of satellites to the central Fe_i^0 line, the ratio of high-field to low-field satellites, and the remarkable dissimilarity in the intensities of the P hyperfine pair lines. The latter phenomenon especially cannot be simulated by assuming a definite geometrical arrangement of P-Fe pairs, which always creates two lines of equal intensities. A further feature which corresponds to the experimental spectra is the asymmetry of the satellite lines.

CONCLUSIONS

In silicon single crystals containing intermediate concentrations of shallow donors and well detectable concentrations of Fe_i^0 a spin-spin interaction between one Fe_i^0 and one neutral donor atom causes a characteristic electron spin resonance spectrum irrespective of the thermal treatment. Thus, one can study the type of interaction between these defects and the local distribution in the samples.

The analysis of our experiments suggests a local distribution of Fe_i^0 ions with respect to neutral shallow donors in FZ and Cz single crystals of silicon, and this distribution is a random one or at least near to it. If there was considerable binding energy, close pairs should have been created in some of the different thermal treatments we did. On the basis of our analysis, such pairs are expected to be detectable if they would exist in an amount assumed in the kinetic experiments recently published.[13] We conclude that processes at room temperature or at elevated temperatures which are passed during "slow quenching" do not produce close pairs of Fe_i^0 and shallow donors to an essential extent. This result, which is all the more valid at high temperature, is important for the discussion of gettering processes.

ACKNOWLEDGMENTS

APPENDIX: FINE STRUCTURE PARAMETER D CAUSED BY A PHOSPHORUS ATOM ON A CUBIC AXIS

The displacement vector u of a P atom in Si is given[23] by

$$u_i = -A_1 \frac{x_i}{r^3} + 3A_3 \left[\frac{x_i^3}{r^5} - \frac{x_i}{r^3} \right]$$
$$- A_3 \left[\frac{2x_i^3}{r^5} + \frac{5x_i}{6r^3} - \frac{5x_i}{r^7} [x_1^4 + x_2^4 + x_3^4] \right], \quad (A1)$$

with

$$A_1 = 4.23 \times 10^{-26} \text{ cm}^3 ,$$

$$A_2 = 5.39 \times 10^{-26} \text{ cm}^3 ,$$

$$A_3 = -3.17 \times 10^{-26} \text{ cm}^3 .$$

Here x_1 to x_3 are the cubic axes. The parameters A_1 to A_3 were calculated from the ratio $C_{12}/C_{11} = 0.383$ of elastic constants of Si and the elastic strength $A = -0.15 \times 10^{-24} \text{ cm}^3$ of P in Si.

The strain field e,

$$e_{jk} = \frac{1}{2} \left[\frac{\partial u_i}{\partial x_k} + \frac{\partial u_k}{\partial x_i} \right] \quad (A2)$$

is related to the stress field by

$$X = C \cdot e , \quad (A3)$$

as usual by the elastic tensor C of Si. The fine structure tensor D can be calculated from

$$D_{jj} = G_{11} \left[X_{jj} - \frac{1}{2} \sum_{j \neq k} X_{kk} \right] , \quad D_{jk} = G_{44} X_{jk} , \quad (A4)$$

with the strain coefficient $G_{11} = -49$ cm^{-1} per unit strain.[5] Locating the defect on a cubic axis yields (11b).

[1]H. Feichtinger, in *Materials Science and Technology*, edited by W. Schröter (VCH Weinheim, New York, 1991), Vol. 4, p. 143.

[2]J. Bailey and E. R. Weber, Phys. Status Solidi A **137**, 515 (1993).

[3]C. A. J. Ammerlaan, in *Numerical Data and Functional Relationships in Science and Technology*, edited by O. Madelung and M. Schulz, Landolt-Börnstein, New Series, Group III, Vol. 22, Pt. b (Springer-Verlag, Berlin, 1989), p. 365.

[4]G. W. Ludwig and H. H. Woodbury, Solid State Phys. **13**, 223 (1962).

[5]M. Berke, E. Weber, H. Alexander, H. Luft, and B. Elschner, Solid State Commun. **20**, 881 (1976).

[6]Y. H. Lee, R. L. Kleinhenz, and J. W. Corbett, Appl. Phys. Lett. **31**, 142 (1977).

[7]W. Gehlhoff and K.-H. Segsa, Phys. Status Solidi A **41**, K21 (1977).

[8]E. Weber and H. G. Riotte, J. Appl. Phys. **51**, 1484 (1980).

[9]E. G. Sieverts, S. H. Muller, C. A. J. Ammerlaan, and E. R. Weber, Solid State Commun. **47**, 631 (1983).

[10]S. Greulich-Weber, J. R. Niklas, E. R. Weber, and J. M. Spaeth, Phys. Rev. B **30**, 6292 (1984).

[11]D. A. van Wezep, T. Gregorkiewicz, E. G. Sieverts, and C. A. J. Ammerlaan, Phys. Rev. B **34**, 4511 (1986).

[12]C. A. J. Ammerlaan, Solid State Phenom. **6/7**, 591 (1989).

[13]H. Takahashi, M. Suezawa, and K. Sumino, Materials Science Forum **143-147**, 1257 (1994).

[14]D. Gilles, Solid State Phenom. **32-33**, 57 (1993).

[15]T. A. Kennedy and J. H. Pifer, Phys. Rev. B **11**, 2017 (1975).

[16]D. New and T. G. Castner, Phys. Rev. B **29**, 2077 (1984).

[17]D. New, Phys. Rev. B **32**, 2419 (1985).

[18]J. H. Pifer, Phys. Rev. B **32**, 7091 (1985).

[19]G. Feher, Phys. Rev. **109**, 1219 (1959).

[20]D. K. Wilson and G. Feher, Phys. Rev. **124**, 1068 (1961).

[21]A. Bencini and D. Gatteschi, *EPR of Exchange Coupled Systems* (Springer-Verlag, Berlin, 1990).

[22]A. Abragam and B. Bleaney, *Electron Paramagnetic Reso-* *nance of Transition Ions* (Clarendon, Oxford, 1970), pp. 151 and 492.

[23]H. Neubrand, Phys. Status Solid B **90**, 301 (1978).

[24]W. Gehlhoff, K. H. Segsa, and C. Meyer, Phys. Status Solidi B **105**, K91 (1981).